Site-directed mutagenesis of multi-copy-number plasmids: Red/ET recombination and unique restriction site elimination

Stephan Noll[1], Gabriele Hampp[1], Hanna Bausbacher[1], Natalia S. Pellegata[2], and Harald Kranz[1]
[1]Gene Bridges GmbH, Heidelberg, Germany and [2]Helmholtz Zentrum München, Institute of Pathology, Neuherberg, Germany

BioTechniques 46:527-533 (June 2009) doi 10.2144/000113150
Keywords: plasmid recombineering, Red/ET recombination, site-directed mutagenesis, unique restriction site elimination

Existing methods for site-directed plasmid mutagenesis are restrained by the small spectrum of modifications that can be introduced by mutagenic primers and the amplicon size limitations of in vitro DNA synthesis. As demonstrated here, the combined use of Red/ET recombination and unique restriction site elimination enables extensive manipulation regardless of plasmid size and DNA sequence elements. First, a selectable marker is PCR-amplified with synthetic primers attaching 50-bp homology target flanks for Red/ET recombination and an arbitrary restriction site absent in the substrate plasmid. The resulting cassette is co-electroporated with substrate plasmids in Red/ET-proficient *Escherichia coli* cells. Following isolation of recombinant plasmids, linear nonselectable DNA replaces the cassette and introduces the desired mutation(s) in a second Red/ET recombination step. Upon selective digestion of parental plasmids and retransformation, a 38% mutation efficiency was achieved using a synthetic 97-nucleotide oligonucleotide to cure a 17-bp deletion within *lacZα* of pUC19 (2,686 bp). A PCR fragment was used with similar efficiency to co-replace mouse *Cdkn1b* codons 9 and 76 in gene-targeting vector pGTC (13,083 bp).

Introduction

Site-directed mutagenesis (SDM) allows DNA modifications by extending oligonucleotide primers which contain the desired mutation(s) flanked by bases complementary to target sequences (1). Several protocols exist in which PCR- and non–PCR-based methods are used (2–8). However, SDM is restrained by the fidelity and template size limitations of in vitro DNA synthesis and the success rate for mutagenesis decreases with the number of mismatches introduced by the mutagnenic primer(s). Hence, an amplicon size–independent method with a broad mutational spectrum would be very useful.

Red/ET recombination has come to be recognized as superior technology for the size and sequence independent manipulation of DNA in *Escherichia coli* (reviewed in Reference 9). The phage λ–derived technology relies on ssDNA or dsDNA fragments with ~50-base tails homologous to the target region. No specific recombination sites are required and homology tails of any sequence can easily be integrated into synthetic oligos either used to PCR-amplify dsDNA flanked by homology or for oligonucleotide-directed recombination. Oligonucleotides complementary to the replicon's lagging strand recombine most efficiently (see Reference 9 and references therein). The Red/ET machinery is composed of exonuclease Redα, which processes linear dsDNA and provides 3′ ss overhangs, and Redβ, which mediates strand annealing and exchange reactions starting from ssDNA extremities. To stabilize dsDNA substrates in the cell, Red/ET recombination is assisted by Redγ, an inhibitor of the host ExoV (see Reference 9 and references therein). For ease of stringent expression control and transfer between strains, we fused the *red* genes to the arabinose-inducible pBAD promoter on thermoreplicative plasmid pRed/ET, which is maintained at ~30°C and lost at temperatures ≥37°C (10).

In genetically stable *E. coli* cells, the recombineering efficiency is ~10^{-4} for dsDNA [e.g., drug resistance (*drug*^{R}) cassettes and ~10^{-3} for oligonucleotides complementary to the replicon's lagging strand] (9). Hence, laborious colony screening is required to detect such an event. Counter-selectable (CS) cassettes have been successfully used in single copy replicons to select for seamless mutants that have undergone recombination leading to its loss (11–14). However, recombineering (recombination-mediated genetic engineering) in a multiple-copy situation results in a mixture of mutated and parental plasmids (15), and phenotypic CS markers are not reliably applicable because a CS gene on a single parental plasmid copy can be sufficient for cell death. In addition, plasmid recombineering facilitates the formation of multimers (15–17). Co-electroporation of modifying linear DNA and substrate plasmids into Red/ET proficient cells was shown to minimize, but not to eliminate, the formation of higher-weight species (15–17).

Here we report a method based on recombineering and unique restriction site elimination (USE), which allows for the efficient and extensive modification of plasmids regardless of size or sequence requirements. *drug*^{R} cassettes were PCR-amplified with primers attaching (*i*) linearization sites (LS) absent in the substrate plasmids, and (*ii*) specific 50-bp target flanks for recombination. Substrate plasmids and *drug*^{R}-LS cassettes were co-electroporated in Red/ET-proficient *E. coli* cells. Upon isolation of recombinant plasmids, modifying ssDNA and dsDNA was used to replace the *drug*^{R}-LS cassettes in a second recombineering step, rendering the mutated plasmids immune to cleavage by USE. Following selective in vitro digestion of parental plasmids and retransformation, a ~38% mutation efficiency was achieved for target plasmids of ≤13 kb.

Materials and methods

E. coli strain and culture conditions

E. coli HS996 (Table 1) was aerobically propagated on Luria-Bertani (LB) broth and agar. As necessary, ampicillin (Ap), chloramphenicol (Cm), kanamycin (Km),

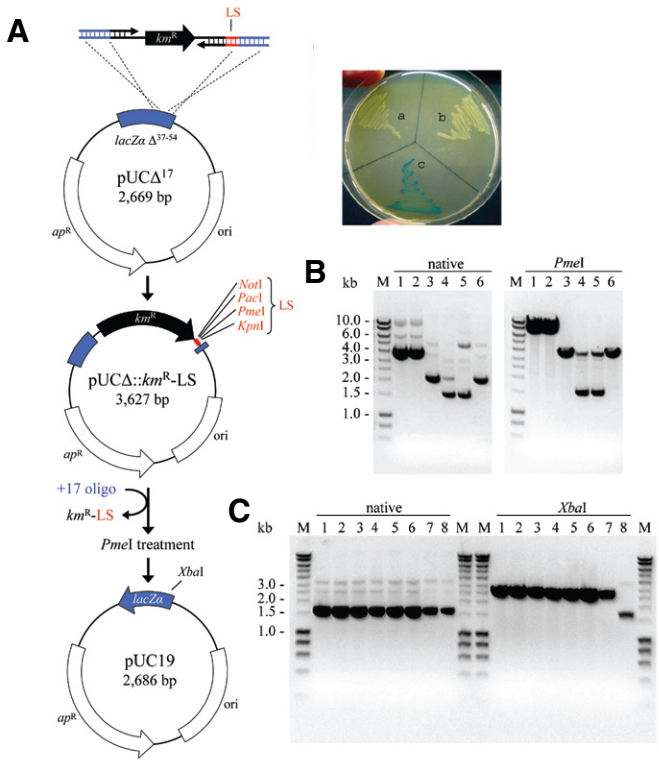

Figure 1. Reconstitution of pUC19. (A) *km*^{R} cassette A002 was PCR-amplified with primers LS1 5′/3′ (small horizontal arrows) which attached 50-base tails homologous to the respective plasmid target sites (blue). In addition, reverse primer LS1 3′ introduced *Kpn*I, *Pme*I, *Pac*I, and *Not*I linearization sites (LS, red). Starting from pUCΔ^{17}, pUC19 was restored in a two-step recombineering approach. In the first step, *km*^{R}-LS (1,057 bp) was inserted at the *lacZ*α deletion site, resulting in pUCΔ::*km*^{R}-LS. Subsequently, *km*^{R}-LS was replaced by oligonucleotide +17 (97 nucleotides), rendering *lacZ*α active in a small subset of plasmids. Recombinant pUC19 plasmids lack the *Kpn*I, *Pme*I, *Pac*I, and *Not*I recognition sites and were ≥500-fold enriched by selective *Pme*I or *Not*I linearization of parental plasmids and retransformation. The relative position of LS sites and the diagnostic *Xba*I site are indicated. Photo, functional analysis of pUC19 restoration. Colonies from *E. coli* pUCΔ^{17} (a), *E. coli* pUCΔ::*km*^{R}-LS (b), and recombined *E. coli* pUC19 (c) were restreaked on a Ap+X-gal indicator plate. *E. coli* pUC19 displayed a blue pigmentation caused by restoration of plasmid-borne *lacZ*α .The photo was taken after overnight incubation at 37°C. (B) Analysis of native and *Pme*I-digested pUCΔ::*km*^{R}-LS candidates isolated from 6 representative Km^R+Ap^R clones. As described previously (15–17), mixed populations of parental and recombined plasmids as well as higher–molecular weight species were observed following recombination. Lanes 3 and 6 displayed mainly supercoiled monomers which appeared as single bands of the expected size (3,627 bp) following *Pme*I treatment. (C) Restriction analysis of recombinant pUC19. All plasmids isolated from seven representative LacZ$^+$ revertants (Ap^R+Km^S) appeared in monomeric state (native, lanes 1–7). Correct oligonucleotide targeting was confirmed by the presence of an *Xba*I site which was used to linearize recombinant pUC19 (*Xba*I, lanes 1–7) whereas original pUCΔ^{17} remained undigested (*Xba*I, lane 8). M, molecular weight marker (HyperLadder I; Bioline, Taunton, MA, USA)

and tetracycline (Tc) were added to final concentrations of 100, 50, 50, and 3 μg/mL, respectively. X-gal (5-bromo-4-chloro-3-indolyl-β-D-galacto-pyranoside; 40 μg/mL) was added to the corresponding plates. Electrocompetent cells for retransformation were prepared as described (18).

DNA manipulations

Standard protocols were used for conventional in vitro cloning (19). HPLC-purified oligonucleotides were obtained from BioSpring (Frankfurt, Germany); *drug*^{R} cassettes A002 (*km*^{R}) and A006 (*cm*^{R}) were purchased from Gene Bridges (Heidelberg, Germany). PCR reactions were performed with Triple Master DNA polymerase according to the manufacturer's recommendations (Eppendorf, Hamburg, Germany). Prior to electroporation, PCR fragments were treated with *Dpn*I and purified using the MinElute PCR purification kit (Qiagen, Hilden, Germany). The QIAprep Spin Miniprep Kit (Qiagen) was used for plasmid isolation. DNA sequencing was done at GATC Biotech (Konstanz, Germany). λ-Red recombination was performed as described by Gene Bridges with minor modifications. In brief, 1.4 mL Red/ET-proficient culture was grown at 30°C to an $OD_{650\ nm}$ of ~0.3. Transient expression of the pRed/ET-encoded *red* genes was induced by adding 50 μL of 10% (w/v) L-arabinose followed by a temperature increase to 37°C. After 25 min, the cells were washed twice with ice-cold 10% (v/v) glycerol and electroporated with DNA in a chilled 1-mm cuvette.

Target plasmids

The target plasmids used in this study are derivatives of high–copy number plasmid pUC19 whose replication origin (ori) initiates mostly unidirectional DNA replication (20). To construct reporter plasmid pUCΔ^{17} (Figure 1A), pUC19 was *Sma*I/*Hinc*II-digested and religated. The 17-bp deletion rendered *lacZ*α inactive (Figure 1A) and resulted in a loss of unique *Bam*HI, *Xba*I, and *Sal*I sites, which was confirmed by sequencing.

pGTC was previously engineered for mouse embryonic stem cell recombination. In brief, a TGG-to-T**A**G point mutation (bold indicates mutation location) of the *mCdkn1b* codon 76 was introduced into BAC RP23–153J19 using *rpsL*-based counter-selection. To achieve pGTC, a 10,446-bp BAC fragment comprising the introduced point mutation was cloned into a pUC19-derived plasmid (2,637 bp).

Results and discussion

km^R-LS construction and targeting of substrate plasmid pUCΔ^{17}

Primers LS1 5′/3′ were designed to PCR-amplify *km*^{R} cassette A002 with 50-base tails homologous to the region flanking the 17-bp deletion within pUCΔ^{17}. In addition, primer LS1 3′ introduced *Kpn*I, *Pme*I, *Pac*I, and *Not*I recognition sites in *km*^{R}-LS (1,057 bp, Figure 1A). Upon co-electroporation of 100 ng *km*^{R}-LS and 10 ng pUCΔ^{17} into Red/ET-proficient cells, we obtained ~300 Ap^R+Km^R transformants. No colonies were observed on selective plates without arabinose induction of the *red* machinery. The migration patterns of potential pUCΔ::*km*^{R}-LS (3,627 bp) isolated from six representative clones were analyzed by gel electrophoresis (Figure 1B). As expected for multiple–copy number plasmids, we observed mixed populations of parental and recombined plasmids as well as higher molecular weight species (15–17). Lanes 3 and 6 were found to contain supercoiled plasmids of mainly monomeric state, which appeared as a single ~3.6-kb band following *Pme*I digestion (Figure 1B). HS996 cells were retransformed with 10 ng of this DNA and correct *km*^{R}-LS integration was confirmed by sequencing.

Reconstitution of pUC19 by oligonucleotide-directed recombination

The oligonucleotide +17, complementary to the lagging strand of pUC19, was designed to have the 17 bases 'missing' in pUCΔ^{17} flanked by an additional 40 bases up- and downstream of the deletion site. We co-electroporated 5 pmol oligonucleotide +17 and 10 ng of pUCΔ::*km*^{R}-LS into Red/ET-proficient HS996. The cells were incubated for 1 h in 1 mL LB at

Table 1. Strains, Plasmids, and Oligonucleotides Used in This Study

	Relevant characteristics/sequences (5′→ 3′)	Reference/source
E. coli		
HS996	F- *mcrA* Δ(*mrr-hsd*RMS-*mcrBC*) φ80*lacZ*ΔM15 Δ*lac*X74 *recA*1 *deoR araD*139 Δ(*ara-leu*)7697 *galU galK rpsL endA*1 *nupG fhuA*::IS2	Gene Bridges
Plasmids		
pRed/ET	*red* expression plasmid, pSC101 based, Tc^R	Gene Bridges
pUC19	cloning plasmid, Ap^R; ColE1 ori	Invitrogen
pUCΔ[17]	pUC19 derivative, Δ*lacZ*α *Sma*I-*Hin*cII, Ap^R	this work
pUCΔ::*km*^{R}-LS	pUC19 derivative, Ap^R, Km^R,	this work
RP23–153J19	pBACe3.6-based, mouse C57BL/J6, Cm^R	Roswell Park, Buffalo, NY, USA
pGTC	gene-targeting vector, pUC19-based, Ap^R, Km^R	this work
pGTC::*cm*^{R}-LS	pGTC derivative, Cm^R	this work
pGTC*	pGTC derivative, GGG-to-**A**GG and TAG-to-T**G**G mutations in *mCdkn1b*, exon 1	this work
Oligonucleotides		**BioSpring**
LS1 5′	CCAGTCACGACGTTGTAAAACGACGGCCAGTGAATTCGAGCTCGGTACCC*TGCAGCAGCACGTGTTGACA*	
LS1 3′	CAGGAAACAGCTATGACCATGATTACGCCAAGCTTGCATGCCTGCAGGTCGGTACCGTTTAAACTTAAT-TAAGCGGCCGC*TCAGACGTCGCTTGGTCGGTCTTTATTCG*	
+17	CTATGACCATGATTACGCCAAGCTTGCATGCCTGCAGGTC**GACTCTAGAGGATCCCC**GGGTACCGAGCTCGAAT-TCACTGGCCGTCGTTTTACAACG	
LS2 5′	GTGGTCCACACCCGCCCGAGGAGGAAGATGTCAAACGTGAGAGTGTCTAACC*AGCACGTGTTGACAATTAATC*	
LS2 3′	CGCGGGGGCCTGTAGTAGAACTCGGGCAAGCTGCCCCTCTCCACCTCCTGGATATCGGCGCGCCGTT-TAAACGGGCCC*TTACGCCCCGCCCTGCCAC*	
PM 5′	*GTGGTCCACACCCGCCCGAGGAGGAAGATGTCAAACGTGAGAGTGTCTAAC***A***GGAGCCCGAGCCT*	
PM 3′	*GCCGGTCCTCAGAGTTTGCCTGAGA*	
GTC1	*TCTGTGTGCAGTCGCAGAAC*	

For all primers listed, nucleotides in blue are homologous to the targeted sequence and those in italic are the PCR primer regions. Endonuclease recognition sites introduced by primers LS1 3′ (*Kpn*I, *Pme*I, *Pac*I, *Not*I) and LS2 3′ (*Eco*RV, *Asc*I, *Pme*I, *Apa*I) are shown in red. Nucleotides introduced or replaced by primers +17 and PM 5′ are shown in bold. ori, replication origin.

37°C and subsequently used to inoculate a 10-mL overnight culture supplemented with Ap. Plasmid DNA (250 ng) isolated from the overnight culture was treated with *Pme*I (10 U in 20 µL, 2 h at 37°C) to selectively linearize parental plasmids, which thereby lose their ability to efficiently transform *E. coli* (21). A control sample without restriction enzyme was incubated under otherwise identical conditions. The samples were heat-inactivated and 25 ng DNA was used to retransform HS996 cells.

*Pme*I treatment resulted in a ~580-fold reduction of Ap^R transformants. Most notably, 38% of the clones obtained from *Pme*I-treated plasmids appeared blue on X-gal indicator plates (Table 2), implying restoration of *lacZα*. A similar result was achieved by using *Not*I for the selective elimination of parental plasmids (data not shown). We restreaked 50 blue colonies on Ap+Km plates. No growth was observed following overnight incubation at 37°C, which demonstrates the complete loss of parental pUCΔ::*km*^{R}-LS plasmids since a single *km*^{R} cassette is sufficient for HS996 to grow at 50 µg/mL Km (data not shown). For seven randomly picked blue clones, pUC19 integrity was inspected by gel electrophoresis (Figure 1C). In all cases examined, the plasmids appeared as monomers and contained the restored *Xba*I site as documented by enzymatic linearization, whereas the original plasmid pUCΔ[17] was immune to *Xba*I cleavage.

Co-generation of scattered point mutations in mouse targeting vector pGTC

To demonstrate the seamless modification of medium- to large-size plasmids without visual color discrimination, we simultaneously introduced two point mutations separated by 200 bp in plasmid pGTC (13,083 bp; Figure 2A). Primers LS2 5′/3′ were designed to amplify *cm*^{R} cassette A006 with 50-base tails homologous to the pGTC region flanking codon 9 to 76 of *mCdkn1b* coding sequence. In addition, LS2 3′ introduced *Apa*I, *Pme*I, *Asc*I, and *Eco*RV recognition sites 3′ of the *cm*^{R} gene (Figure 2A). Upon co-electroporation of 100 ng *cm*^{R}-LS (863 bp) and 10 ng pGTC into Red/ET-proficient cells, we obtained 112 Cm^R transformants. No colonies were observed on selective plates without arabinose-induction of the recombination machinery. Plasmids were isolated from 10 transformants and migration patterns were analyzed by gel electrophoresis (Figure 2B). We found 8 clones to appear mainly as monomers. *Sca*I digestion revealed migration patterns characteristic for various populations of parental and recombinant plasmids. We retransformed HS996 with 10 ng of mainly monomeric recombinant plasmid DNA to separate pGTC::*cm*^{R}-LS from traces of parental pGTC and higher-weight species.

Primers PM 5′/3′ were used to PCR-amplify a 412-bp fragment from original BAC RP23–153J19 (Figure 2A). PM 5′ introduced a GGG-to-**A**GG point mutation corresponding to codon 9, whereas the codon exchange at position 76 (TAG-to-T**G**G) reflected a reversion to the BAC-encoded wild-type situation. Codons 9 and 76 of the modifying DNA were flanked by 50-bp and 156-bp tails homologous to *mCdkn1b*. Thus, the PCR fragment enabled us to co-introduce codon exchanges at position 9 and 76 of pGTC-borne *mCdkn1b*. We co-electroporated 100 ng PCR product and 10 ng pGTCΔ::*cm*^{R}-LS into Red/ET proficient HS996. Afterwards, the cells were treated as described for the pUC19 reconstitution except that overnight incubation was performed in the presence of Ap+Km and *Apa*I (10 U) was used for USE. Following *Apa*I digestion we obtained 20 colonies on Ap+Km plates, while ~10,000 transformants were received without enzymatic treatment. Nine out of the 20 clones were found to be Cm^S, implying loss

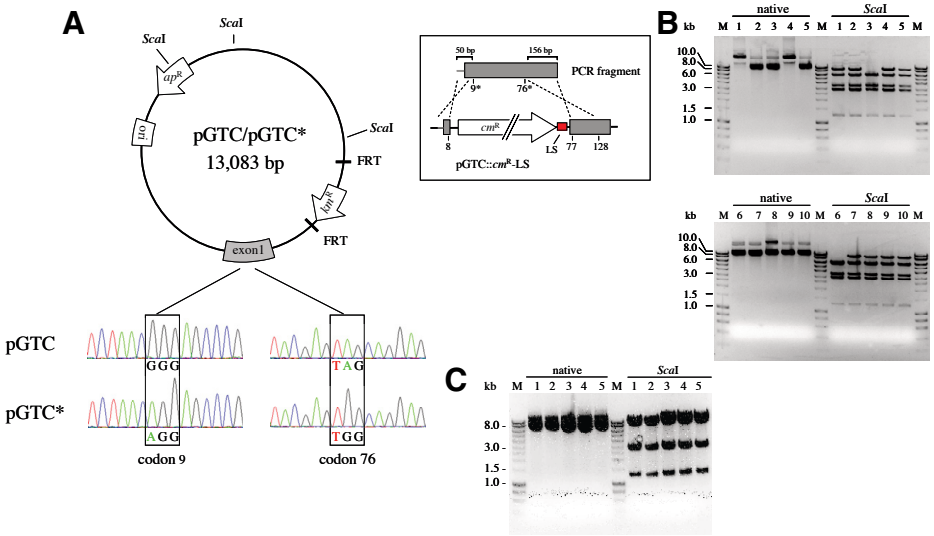

Figure 2. Simultaneous generation of point mutations in codon 9 and codon 76 of the pGTC-borne mCdkn1b exon 1. (A) Schematic map of pGTC and mutated pGTC* (13,083 bp). The relative positions of diagnostic *Sca*I recognition sites are indicated. The codon exchanges within exon 1 of *mCdkn1b* at position 9 (GGG-to-**A**GG) and position 76 (TAG-to-T**G**G) were confirmed by sequencing using primer GTC1 (Table 1) The box indicates the second recombineering step. PCR-fragment tails 5′ of codon 9* (**A**GG) and 3′ of codon 76* (T**G**G) share 50- and 156-bp sequence homology with target plasmid pGTC::*cm*^{R}-LS. (B) Analysis of native and *Sca*I-digested pGTC::*cm*^{R}-LS candidates isolated from 10 representative Ap^R+Cm^R+Km^R clones. Upon targeting pGTC with PCR-amplified *cm*^{R}-LS (863 bp), mainly monomeric species formed. The *Sca*I digestion patterns revealed various mixtures of parental pGTC (8,778 bp, 2,998 bp, 1,307 bp) and recombinant pGTC::*cm*^{R}-LS (5,907 bp, 3,429 bp, 2,998 bp, 1,307 bp), whereas the majority of plasmids in lanes 3 and 6 are the desired molecules. Retransformation was performed with 10 ng plasmid DNA shown in lane 3 to separate it from traces of parental plasmids and multimers. (C) Restriction analysis of recombined pGTC*. Plasmids isolated from 5 Ap^R+ Km^R+Cm^S clones appeared as monomers in their native state and displayed the expected *Sca*I digestion patterns (8,778 bp, 2,998 bp, 1,307 bp) characteristic for recombinant plasmids. Partial sequencing of all 5 plasmids with primer GTC1 confirmed the introduction of the desired point mutations. FRT, FLP recognition target sites; LS, linearization sites; M, molecular weight marker (HyperLadder I, Bioline).

Table 2. Mutation Efficiency for the Reconstitution of pUC19 by Oligonucleotide-directed Recombination, USE, and Retransformation

Phenotype	Colony no.	
	*Pme*I-digested	Undigested
blue	112 ± 11	—
white	184 ± 51	171,000 ± 12,000
	∑ 296 ± 62	∑ 171,000 ± 12,000

Upon targeting pUCΔ::*km*^{R}-LS with oligonucleotide +17, *Pme*I-digested or undigested plasmid DNA (25 ng) isolated from Ap^R cells was used to retransform HS996. LB plates supplemented with Ap and X-gal were used to determine the number of transformants following overnight incubation at 37°C. The values are the mean and standard deviation of three independent digestion and transformation experiments. Cells transformed with undigested plasmids were diluted 1:1000 prior to plating.

of the plasmid-borne *cm*^{R}-LS cassette. Native and *Sca*I-digested plasmids from 5 representative Ap^R+Km^R+Cm^S clones revealed the predicted migration pattern for monomeric pGTC* (Figure 2C). Sequencing confirmed the expected GGG-to-**A**GG (codon 9) and TAG-to-T**G**G (codon 76) exchanges (Figure 2A).

Based on previous work (15–17,22) we have developed a recombineering protocol to introduce seamless mutations onto high–copy number plasmids. As described here, two rounds of recombination enabled precise and scarless plasmid manipulations (i.e., the restoration of pUC19 by oligonucleotide +17 and the co-introduction of scattered point mutations in gene-targeting vector pGTC. While we have focused on ColE1-based plasmids in this study, our unpublished results show that this method is also applicable for the manipulation of p15A-based vectors.

Using genetically stable *E. coli* HS996, we expected the plasmid recombination frequency to be in the range of their BAC and chromosomal counterparts (i.e., ~10^{-3}–10^{-4}) (9). Strain and/or culturing condition-specific CS markers like *rpsL*, *sacB*, *thyA*, and *tolC* have been successfully used to identify recombinant single-copy replicons where the counterselective cassette was replaced by markerless DNA (11–14). However, we expected these CS markers to cause problems in plasmid recombineering where the bulk of transformants contain plasmid mixtures (15). For that reason, we have applied a rational USE approach to selectively eliminate parental plasmids in vitro. Deng and Nickoloff originally combined USE and SDM (8). The novelty of using USE here is that any restriction site a priori absent in the original vector can be chosen for plasmid linearization. This approach is of broad application because a 'non-cutting' enzyme is usually available even for a large plasmid. Thus, a site-specific *drug*^{R}-LS cassette can be designed, PCR-amplified, and introduced in almost any substrate plasmid, which then gets tagged for seamless downstream manipulation.

We found the isolation of monomeric *drug*^{R}-LS encoding plasmids to be critical for the success of the whole strategy. Co-electroporation of substrate plasmids and modifying DNA minimized the formation of multimers and resulted mainly in populations of monomeric parental and recombinant plasmids as displayed by gel electrophoresis (Figures 1B, 2B). In contrast, targeting resident pUCΔ[17] with *km*^{R}-LS yielded higher weight molecules—most likely dimers—as the dominant species (data not shown). Thus, the isolation of monomeric *drug*^{R}-LS plasmids requires careful monitoring of the plasmid topology and retransformation to purify desired monomeric molecules away from parental plasmids and multimers.

Targeting pUCΔ::*km*^{R}-LS and pGTC::*cm*^{R}-LS with linear ss or ds modifying DNA was followed by USE. This step is directly correlated to the success of mutagenesis because linear plasmid is about 10^3–10^4 times less efficient in electroporating *E. coli* than its corresponding circular plasmid (21). Hence, recombinant plasmids were enriched ≥500-fold by selective *Pme*I, *Not*I, or *Apa*I digestion and retransformation. Although we did not achieve a quantitative elimination of parental pUCΔ::*km*^{R}-LS plasmids, our results indicate that the vast majority of blue transformants obtained on Ap+X-gal plates were LacZ$^+$ revertants which contained monomeric recombinant pUC19 and did not harbor parental plasmids (Figure 1C). No multimers were observed after the second recombination

step (Figures 1C and 2C), which suggests that higher-weight species still contain a parental allele and are subject to USE. Thus, we divided the number of blue colonies by the total number of colonies (Table 2) to calculate a recombination frequency of ~7×10^{-4} for the oligonucleotide-directed reconstitution of pUC19. Since there is no selection pressure on the mutagenic +17 oligonucleotide, this reflects an objective indication of the plasmid recombineering process in genetically stable cells. Recombinant pGTC* (Figure 2) was obtained with similar efficiency which demonstrates that no visual discrimination is required to rapidly identify desired plasmids.

Conclusions

Plasmid recombineering opens access to an extensive mutational spectrum because this method is suitable to introduce single or multiple scarless modifications (insertion, deletion, replacement) in a wide range of sizes. In contrast, SDM methods usually tolerate only a few mismatches in the mutagenic primer. Furthermore, several protocols depend on methyl-directed mismatch repair (MMR)–deficient host strains to prevent in vivo repair of the unmethylated newly synthesized DNA strand (23,24). The drawback here is that silencing the MMR system significantly reduces the replication fidelity (25).

Our method does not require in vitro amplification of the plasmid backbone or the use of a mutagenic *E. coli* host strain. Thus, even large plasmids can be manipulated without the risk of accumulating random mutations. The superior flexibility of recombineering also has definite advantages for the manipulation of small plasmids, which are accessible by existing methodology. For example, plasmids designed for heterologous protein production and purification (e.g., pQE and pET series) can be directly targeted with PCR-amplified or synthetic genes that thereby replace the multiple cloning site. This is likely to provide one or more restriction enzyme candidates for the elimination of empty parental vectors. Since the base-precise join points of the recombinant plasmid are defined by the arbitrary sequence of the target gene flanks, plasmid recombineering—which dispenses with the need for intermolecular ligation—overcomes problems associated with in-frame cloning and the addition of unwanted 5′ or 3′ codons.

Given its flexibility and relative ease, the method reported here should prove to be a welcome alternative to conventional methods of plasmid manipulation.

Acknowledgments

We thank our coworkers in the laboratory for testing our protocol. We are grateful to A. Francis Stewart for helpful discussions. The authors thank Michaela Biener, Saskia Lösch, and Verena Schwarz for excellent technical assistance. N.S.P. is funded by EU grant no. LSHG-2006-037188.

S.N., G.H., H.B., and H.K. are employees of Gene Bridges GmbH.

References

1. **Smith, M.** 1985. In vitro mutagenesis. Annu. Rev. Genet. *19*:423-462.
2. **Higuchi, R., B. Krummel, and R.K. Saiki.** 1988. A general method of in vitro preparation and specific mutagenesis of DNA fragments: study of protein and DNA interactions. Nucleic Acids Res. *16*:7351-7367.
3. **Shimada, A.** 1996. PCR-based site-directed mutagenesis. Methods Mol. Biol. *57*:157-165.
4. **Ho, S.N., H.D. Hunt, R.M. Horton, J.K. Pullen, and L.R. Pease.** 1989. Site-directed mutagenesis by overlap extension using the polymerase chain reaction. Gene *77*:51-59.
5. **Horton, R.M., H.D. Hunt, S.N. Ho, J.K. Pullen, and L.R. Pease.** 1989. Engineering hybrid genes without the use of restriction enzymes: gene splicing by overlap extension. Gene *77*:61-68.
6. **Sarkar, G. and S.S. Sommer.** 1990. The "megaprimer" method of site-directed mutagenesis. BioTechniques *8*:404-407.
7. **Zoller, M.J. and M. Smith.** 1982. Oligonucleotide-directed mutagenesis using M13-derived vectors: an efficient and general procedure for the production of point mutations in any fragment of DNA. Nucleic Acids Res. *10*:6487-6500.
8. **Deng, W.P. and J.A. Nickoloff.** 1992. Site-directed mutagenesis of virtually any plasmid by eliminating a unique site. Anal. Biochem. *200*:81-88.
9. **Sawitzke, J.A., L.C. Thomason, N. Costantino, M. Bubunenko, S. Datta, and D.L. Court.** 2007. Recombineering: in vivo genetic engineering in *E. coli, S. enterica*, and beyond. Methods Enzymol. *421*:171-199.
10. **Zhang, Y., J.P. Muyrers, G. Testa, and A.F. Stewart.** 2000. DNA cloning by homologous recombination in *Escherichia coli*. Nat. Biotechnol. *18*:1314-1317.
11. **Warming, S., N. Costantino, D.L. Court, N.A. Jenkins, and N.G. Copeland.** 2005. Simple and highly efficient BAC recombineering using *galK* selection. Nucleic Acids Res. *33*:e36.
12. **Wong, Q.N., V.C. Ng, M.C. Lin, H.F. Kung, D. Chan, and J.D. Huang.** 2005. Efficient and seamless DNA recombineering using a thymidylate synthase A selection system in *Escherichia coli*. Nucleic Acids Res. *33*:e59.
13. **DeVito, J.A.** 2008. Recombineering with *tolC* as a selectable/counter-selectable marker: remodeling the rRNA operons of *Escherichia coli*. Nucleic Acids Res. *36*:e4.
14. **Heermann, R., T. Zeppenfeld, and K. Jung.** 2008. Simple generation of site-directed point mutations in the *Escherichia coli* chromosome using Red/ET recombination. Microb. Cell Fact. *7*:14.
15. **Thomason, L.C., N. Costantino, D.V. Shaw, and D.L. Court.** 2007. Multicopy plasmid modification with phage lambda Red recombineering. Plasmid *58*:148-158.
16. **Zhang, Y., F. Buchholz, J.P. Muyrers, and A.F. Stewart.** 1998. A new logic for DNA engineering using recombination in *Escherichia coli*. Nat. Genet. *20*:123-128.
17. **Yu, D., H.M. Ellis, E.C. Lee, N.A. Jenkins, N.G. Copeland, and D.L. Court.** 2000. An efficient recombination system for chromosome engineering in *Escherichia coli*. Proc. Natl. Acad. Sci. USA *97*:5978-5983.
18. **Dower, W.J., J.F. Miller, and C.W. Ragsdale.** 1988. High efficiency transformation of *E. coli* by high voltage electroporation. Nucleic Acids Res. *16*:6127-6145.
19. **Sambrook, J. and D.W. Russell.** 2001. Molecular Cloning: A Laboratory Manual, 3rd ed. CSH Laboratory Press, Cold Spring Harbor, NY.
20. **Inselburg, J.** 1974. Replication of colicin E1 plasmid DNA in minicells from a unique replication initiation site. Proc. Natl. Acad. Sci. USA *71*:2256-2259.
21. **Shigekawa, K. and W.J. Dower.** 1988. Electroporation of eukaryotes and prokaryotes: a general approach to the introduction of macromolecules into cells. BioTechniques *6*:742-751.
22. **Thomason, L., D.L. Court, M. Bubunenko, N. Costantino, H. Wilson, S. Datta, and A. Oppenheim.** 2007. Recombineering: genetic engineering in bacteria using homologous recombination. *In* Current Protocols in Molecular Biology, John Wiley and Sons, New York.
23. **Kramer, B., W. Kramer, and H.J. Fritz.** 1984. Different base/base mismatches are corrected with different efficiencies by the methyl-directed DNA mismatch-repair system of *E. coli*. Cell *38*:879-887.
24. **Zell, R. and H.J. Fritz.** 1987. DNA mismatch-repair in *Escherichia coli* counteracting the hydrolytic deamination of 5-methyl-cytosine residues. EMBO J. *6*:1809-1815.
25. **Schofield, M.J. and P. Hsieh.** 2003. DNA mismatch repair: molecular mechanisms and biological function. Annu. Rev. Microbiol. *57*:579-608.

Received 13 January 2009; accepted 17 March 2009.

Address correspondence to Stephan Noll, Gene Bridges GmbH, Im Neuenheimer Feld 584, 69120 Heidelberg, Germany. e-mail: stephan.noll@genebridges.com